

# Effect of producer gas addition on spectral characteristics of the natural gas flame

---

**Andrius Saliamonas,**

**Robertas Navakas,**

**Nerijus Striūgas,**

**Algis Džiugys,**

**Kęstutis Zakarauskas**

*Laboratory of Combustion Processes,  
Lithuanian Energy Institute,  
Breslaujos St. 3, LT-44403 Kaunas,  
Lithuania  
E-mail: Andrius.Saliamonas@lei.lt*

The aim of this article is to show the results of investigation how mixing producer gas (PG) (a product of a biomass gasification process) into the natural gas (NG) flow affects spectral characteristics of flame at specific wavelengths, representing formation reactions of  $\text{OH}^*$ ,  $\text{CO}^*$  and  $\text{C}_2^*$  radical species, when the air equivalence ratio (ER) ranges from 1.0 to 1.3. In the current research, experiments were carried out for natural gas and mixtures of natural gas and producer gas. The producer gas was generated from wood pellets in a lab scale gasification reactor. Conventional flame emission spectroscopy methods were used for combustion process monitoring and control. This article presents the results of flame analysis by the emission spectroscopy method for registering chemiluminescent radical species  $\text{OH}^*$ ,  $\text{CH}^*$  and  $\text{C}_2^*$ . After analysing the profile shape of chemiluminescent species intensity distribution along the burner vertical axis, it was determined that the quenching effect takes part in the combustion zone at some specific conditions. Additionally, the shift of chemiluminescence intensity towards the burner nozzle was registered when natural gas was mixed with producer gas. This effect was due to the presence of hydrogen in the producer gas.

**Key words:** producer gas, combustion, chemiluminescence, renewable energy sources, spectroscopy

---

## INTRODUCTION

Partial or full substitution of natural gas (NG) with producer gas (PG) from waste or renewable sources is becoming a common practice nowadays; therefore, identification of trends in combustion of this type of fuel mixtures is important for developing both the burners, and monitoring and control systems. In the past decade, the usage of chemiluminescence in creation of active combustion process management systems made a great progress. During this time, the main methods of analysis were developed for processing the data acquired by non-intrusive optical monitoring. Currently, the most common tools for such research are the Cassegrain optical systems, reconstruction of 3D structure of flame by

using inverse Abel transformation or 3D topography algorithms and use of Planar Laser Induced Fluorescence (PLIF) [1]. Depending on a specific problem, each of these methods has some advantages and also some drawbacks. For example, PLIF is most successfully applied in small particle tracking, but it is also applicable for chemiluminescence research. The downside of this technique is that equipment is relatively expensive and applicable mostly for laboratory research. Also it is known that the ground state  $\text{OH}^*$  radicals, which are abundant in the post-flame gas reaction zone, can be excited by PLIF, and this can generate errors in research. This problem does not apply when using Cassegrain (CS) optics because it detects only the natural chemiluminescence in the reaction zone [2]. The inverse Abel transform

and 3D topography methods may be the least expensive methods for analyzing data, since a single projection (such as a single camera image) is sufficient assuming the flame is axially symmetric; therefore, they require very steady and symmetrical flame [3]. Despite the mentioned minor drawbacks, these techniques are known as essential for collecting data related to flame chemiluminescence and are acceptable by the scientific society.

A number of studies on spectral imaging of hydrocarbon flames have been published. Har-dalupas and Orain et al. [4] used natural gas with 94% methane and air that were premixed and subsequently injected with a symmetrical flow in opposing jets through four pipes, parallel to the axis of the burner. The results of investigation stated that intensities of chemiluminescence from  $\text{OH}^*$  and  $\text{CH}^*$  and the background intensity from  $\text{CO}_2^*$  are able to indicate the heat release rate, whereas that from  $\text{C}_2^*$  is not. It was also found that the ratio of intensities  $\text{OH}^*/\text{CH}^*$  has a monotonic decrease with the equivalence ratio for lean and stoichiometric mixtures, while remaining independent of the flame strain rate. This leads to the conclusion that it is possible to measure the equivalence ratio of the reacting mixture using the intensity of chemiluminescence. Veríssimo and Rocha et al. [5] based on the  $\text{OH}^*$  images reported that as the excess air coefficient increases the main reaction zone moves progressively closer to the burner presumably due to a faster entrainment of fuel and burnt gases, and due to the increase in the oxygen concentration in the recirculated flue-gas. Bouvet and Chauveau et al. [6] commented that the volumetric heat loss and collisions of active radical species are dependent on the burner tube diameter and increase with the increase of diameter. This is why producer gas flames in their research with  $\text{H}_2 < 20\%$  could not be sustained at the open end of the 4 mm diameter tube, while stable flames could be obtained on the 12 mm burner for the same mixture compositions. They also noted that the flame stability regions can be considerably extended towards lower air equivalence ratio values when using methane / air pilot flame. Higgins and McQuay [7] added that the  $\text{OH}^*$  emission decreased significantly with the increasing pressure. In their research the  $\text{OH}^*$  emission also monotonically increased with

the equivalence ratio decrease, and a linear relationship was observed between the increasing mass flow and increasing chemiluminescence as in [4]. Therefore, it was concluded that a suitable resolution and dynamic range exist for a high-pressure flame to be adequately controlled to minimize both  $\text{NO}_x$  and CO emissions.

Ballester and García-Armingol et al. [8] concluded that the chemiluminescent light emitted is directly proportional to the concentration of the excited radical, which is a result of its formation and destruction rates. The obtained main kinetic reaction pathways and the wavelengths corresponding to the chemical reaction are presented in Table 1. For example, based on Higgins and McQuay et al. [9], the excited state radical  $\text{CH}^*$  is produced primarily through the reaction of  $\text{C}_2\text{H}$  with molecular oxygen. The resulting excited  $\text{CH}^*$  loses its energy either through a physical quenching (i. e. collisions) or spontaneous fluorescence (i. e. chemiluminescence). This chemiluminescence can be registered at a wavelength of 430 nm.

Table 1. Wavelengths related to main chemiluminescent radical formation reactions [8]

Radical	Reaction	Wavelength, nm
$\text{OH}^*$	$\text{CH} + \text{O}_2 \rightarrow \text{CO} + \text{OH}^*$	282.9, 308.9
$\text{CH}^*$	$\text{C}_2\text{H} + \text{O}_2 \rightarrow \text{CO}_2 + \text{CH}^*$	387.1, 431.4
$\text{C}_2^*$	$\text{CH}_2 + \text{C} \rightarrow \text{C}_2^* + \text{H}_2$	513, 516.5

According to this information, five optical filters with various band-pass were used for flame imaging in the experiments presented in the current article. Filter properties are described in the Methodology chapter. The wavelengths of these filters represent the reactions mentioned in Table 1 because these reactions are considered to be the leading ones in the combustion process.

The aim of this article is to present the results of an experimental analysis of the change of spectral characteristics of the premixed natural and producer gas flame at  $\text{OH}^*$ ,  $\text{CO}^*$  and  $\text{C}_2^*$  wavelength ranges for different air equivalence ratio (ER) ranging from 1.0 to 1.3. According to the experimental results, we determined whether the already known tendencies for air equivalence ratio relation to  $\text{OH}^*/\text{CH}^*$  ratio are applicable for gas that was produced from biomass. Producer gas was generated from woodchips, since the

woodchips are one of the most common forms for biomass used for energy production.

## METHODOLOGY

### Experimental setup

The experiments were performed using the experimental setup shown in Fig. 1. It consists of an air / gas supply system, a gasification reactor system for producer gas supply, a combustion chamber, and a flame optical analysis system. All supply systems (Air, PG and NG) were connected to the combustion chamber. For each measurement of flame chemiluminescence, an initial volumetric gas flow was set with flow meters.

The combustion chamber was made of a 56 cm height and 6 cm diameter transparent quartz glass pipe. The pipe was mounted on a metal stand, which connects the combustion chamber and the premixed gas burner. Natural gas and primary air flows were connected to the burner via rubber tubing. Mixing of both flows occurred inside the burner. The combustion chamber had a circular hole with a diameter slightly bigger than that of the

burner. The remaining gap was used for secondary air flow supply into the combustion chamber. At the top of the combustion chamber, a flue gas analyzer TESTO 350 XL probe was inserted at a 50 cm distance from the burner.

During the experiment, producer gas and natural gas mixtures were used with a well-defined composition (Table 2).

Producer gas was generated by using a lab scale gasification reactor, which was described in detail elsewhere [10] (8; when referring to components of the experimental setup, the numbers correspond to Fig. 1). Producer gas was generated by the following procedures:

Nitrogen flow (1.8 l/min) for pyrolysis gas transportation was supplied into a container filled with fuel pellets. Pellets made from a mix of pine and spruce wood were used for the experiments. The pellet properties are given in Table 3.

The entire combustion process was observed by an optical system, which produced the 2D images for  $\text{OH}^*$ ,  $\text{CH}^*$  and  $\text{C}_2^*$  spatial distribution in flame at atmospheric pressure. For capturing images, the Andor iStar ICCD (Intensified Charge Coupled

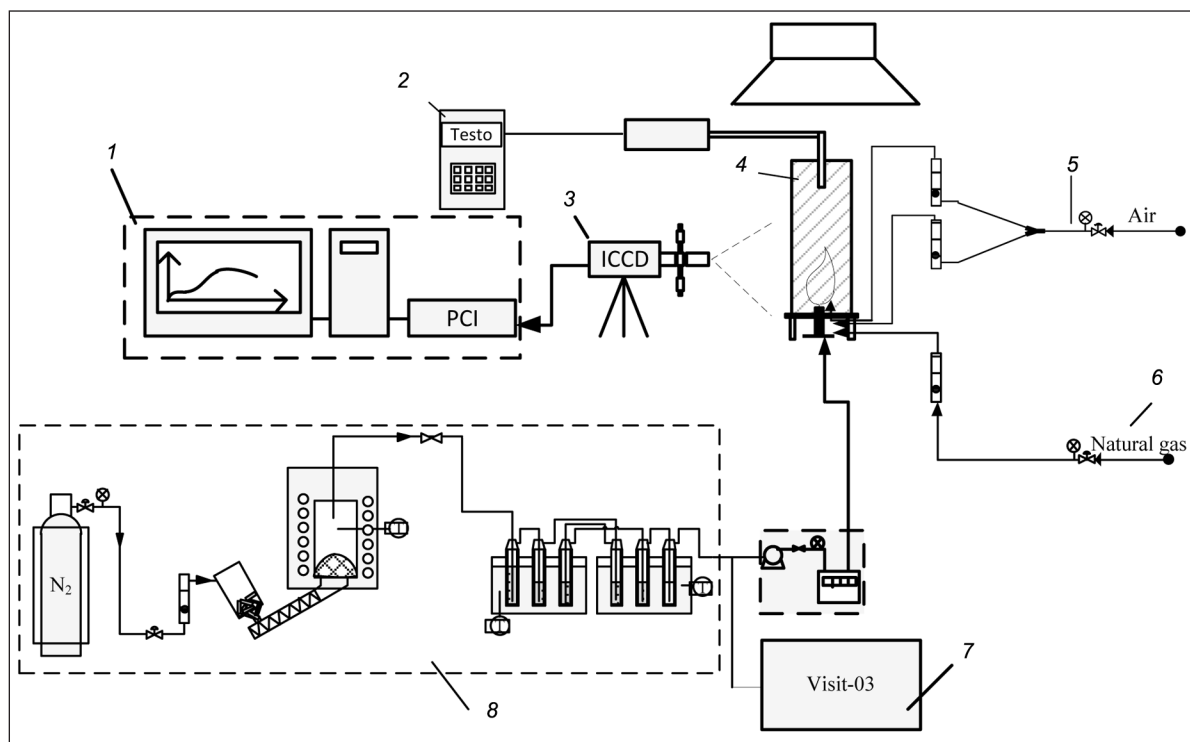


Fig. 1. Experimental setup: 1 – computer with spectroscopic data analysis software; 2 – flue gas analyser TESTO 350 XL; 3 – ICCD camera with optical filters; 4 – combustion chamber; 5 – air supply system; 6 – natural gas supply system; 7 – producer gas composition analyser; 8 – producer gas generation system

Table 2. Inlet parameters for fuel and air flows

Producer gas	Natural gas	Producer gas	Air flow			
In mixture	Flow	Flow	ER = 1.0	ER = 1.1	ER = 1.2	ER = 1.3
%	l/min	l/min	l/min	l/min	l/min	l/min
0	1.08	0	10.30	11.33	12.37	13.40
20	0.86	0.80	9.94	10.93	11.93	12.92
35	0.70	1.40	9.67	10.63	11.60	12.57

Table 3. Properties of wood pellets used in the experiment

Ash, wt.%	Moisture content	Lower calorific value, MJ/kg	Wood composition, wt.% dry				
			C	H	O	N	S
0.35	5.20	19.00	49.20	6.20	44.46	0.08	0.06

Device) camera was used. The 18 mm-sized sensor consisted of  $1024 \times 1024$  pixels sensitive to 200–800 nm wavelength light. The resolution achieved was 6.6 pixel/mm. The ICCD camera was operated with the Solis software. Optimal exposure was set to 01.s, and 300 frames were accumulated into a single frame for each flame condition and each optical filter. Single accumulation cycle time was set to 1.266 s (Fig. 2). Multiple frames were recorded for each combustion and imaging regime (fuel mixture composition, fuel and air flow rates, selected optical filter) in order to minimize the effect of flame instability.

For registering individual species, five optical filters were used. Filters were chosen according to wavelengths related to the main chemiluminescent radical formation reactions, mentioned in Table 1. The parameters of optical filters used in the experiments are given in Table 4.

The prepared producer gas was then supplied through a separate channel into the burner. The flow was controlled by a Zambelli ZB1 suction pump (max flow rate free inlet 30 l/min; max vacuum >580 mmHg; operating range 0.4–30 l/min). Air flow was supplied by two separate channels. Both air flows were controlled by flow meters (operating range 0.5–20 l/min). Primary air was mixed with the gas flow inside the burner. Se-

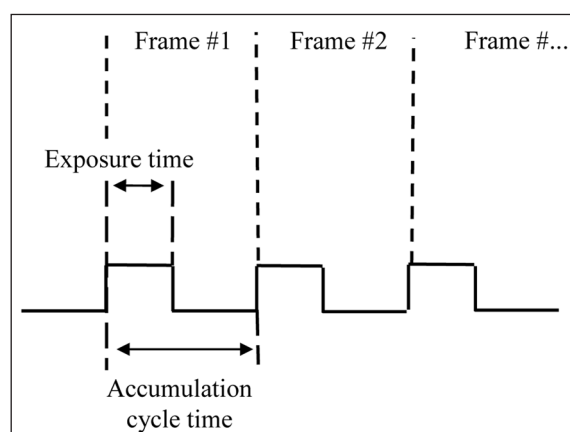


Fig. 2. Image acquisition timing scheme

condary air was used for flame stabilization, and it was flowing into the burning chamber through a gap between the burner and the metal stand. Experiments were performed for ER 1.0, 1.1, 1.2 and 1.3 while maintaining the constant 0.6 kW output for the mixture (see Table 2).

### Data processing

To reduce flame instability for each flame condition and each filter, 300 frames were put together with the Solis software resulting in a single image representing the mean values of species spatial dis-

Table 4. The parameters of optical filters used in the experimental investigation

Filter No.	Radical	Wavelength	Transparency
1, 4	CH*	431.1 nm, 387.1 nm	>95%, >90%
2	C2*	514 nm	>65%
3, 5	OH*	308.9 nm, 282.9 nm	>15%, >65%

tribution. To filter out the camera internal noise, a dark frame was taken with a capped camera, and the values of this frame were subtracted from the main image. The dark frame was taken with a photocathode set to “off” and the camera was covered with cloth to prevent accidental light leaks during exposure.

Collected raw data were saved via Flexible Image Transport System (FITS) files and were imported into the MATLAB environment for further processing. In order to determine how light intensity changes along the combustion chamber in a vertical direction, each horizontal line of pixel intensity values in the frame being analyzed was averaged, thereby producing the averaged distri-

bution of chemiluminescence intensity along the flame axis, representing relative concentrations of chemiluminescent species along the burner axis. In parallel, the total mean intensity values of each image were calculated in order to compare how the total intensity of chemiluminescence changes with changing ER.

## RESULTS AND DISCUSSION

The unprocessed flame images were collected and compared. Different distribution of intensity was observed in each image taken with different optical filter and with different flame condition (Fig. 3), so further analysis was done.

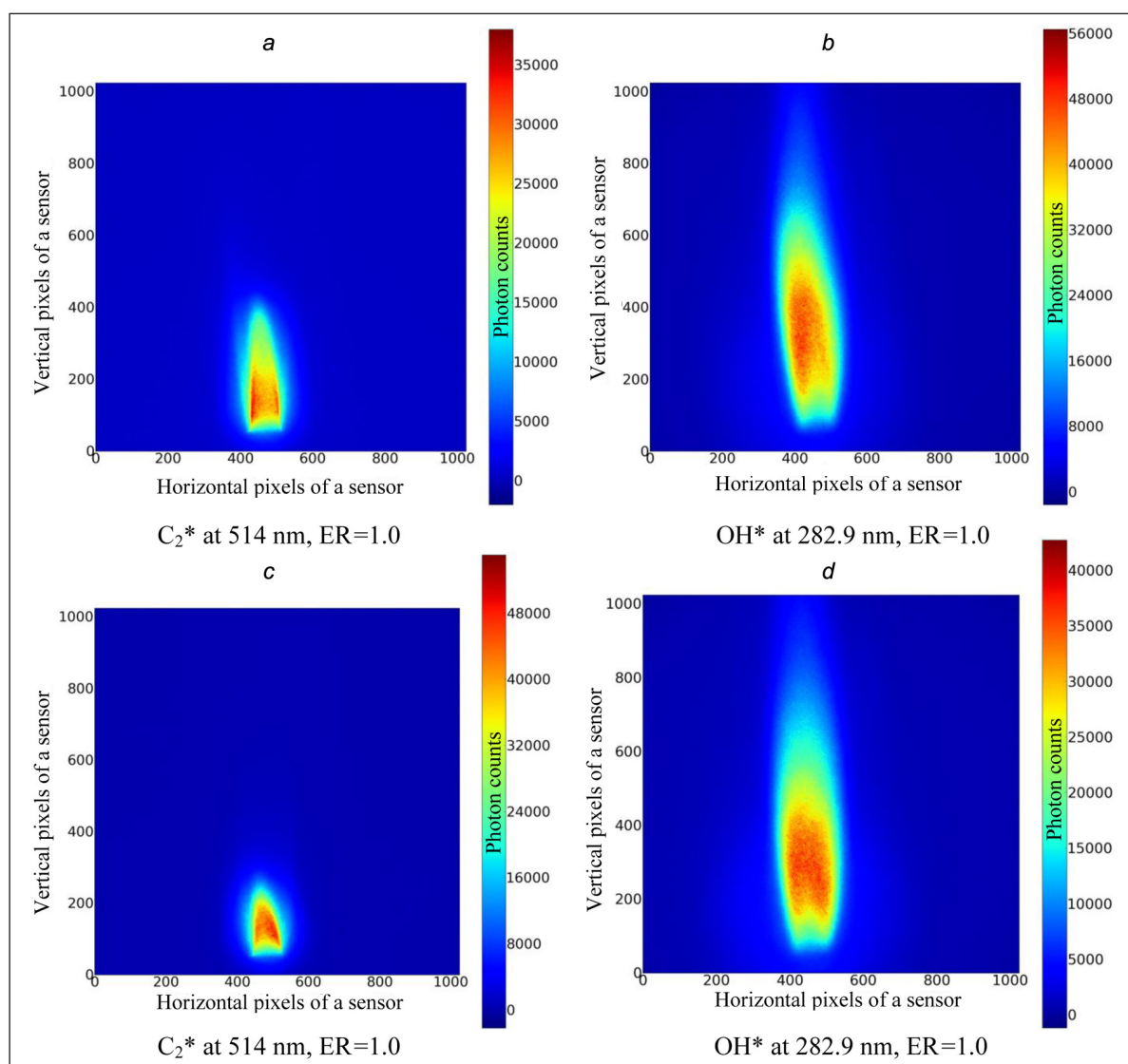


**Fig. 3.** Unprocessed flame images taken through different optical filters: *a, b* – 100% natural gas; *c, d* – natural gas 65%, producer gas 35%. The images are in false colours: the colour corresponds to the photon counts at the respective wavelength on the respective pixels of the CCD matrix



The results show that the spectral intensity along the flame has similar profile shapes at 431.4 nm ( $\text{CH}^*$ ), 514 nm ( $\text{C}_2^*$ ), and 282.9 nm ( $\text{OH}^*$ ) wavelengths (Fig. 3). Similar results were obtained by other authors, who used the same or similar experimental methodology [3, 11]. At described wavelengths, two peaks of spectral intensity were observed at 1 cm and 3–5 cm distance from the burner nozzle (Fig. 3a). Observed peaks correspond to chemical reactions related

to the spectral intensity at a specific wavelength (see Table 1). According to Hardalupas et al. [2], only the maximum intensity values are important when deciding about the chemical reaction at a defined point in space, and the areas before and after the peaks are considered as reaction beginning and ending zones. Stable increasing and decreasing of  $\text{OH}^*$  and  $\text{CH}^*$  intensity was observed only at two wavelengths (308.9 and 387.1 nm) (Fig. 4b, c).

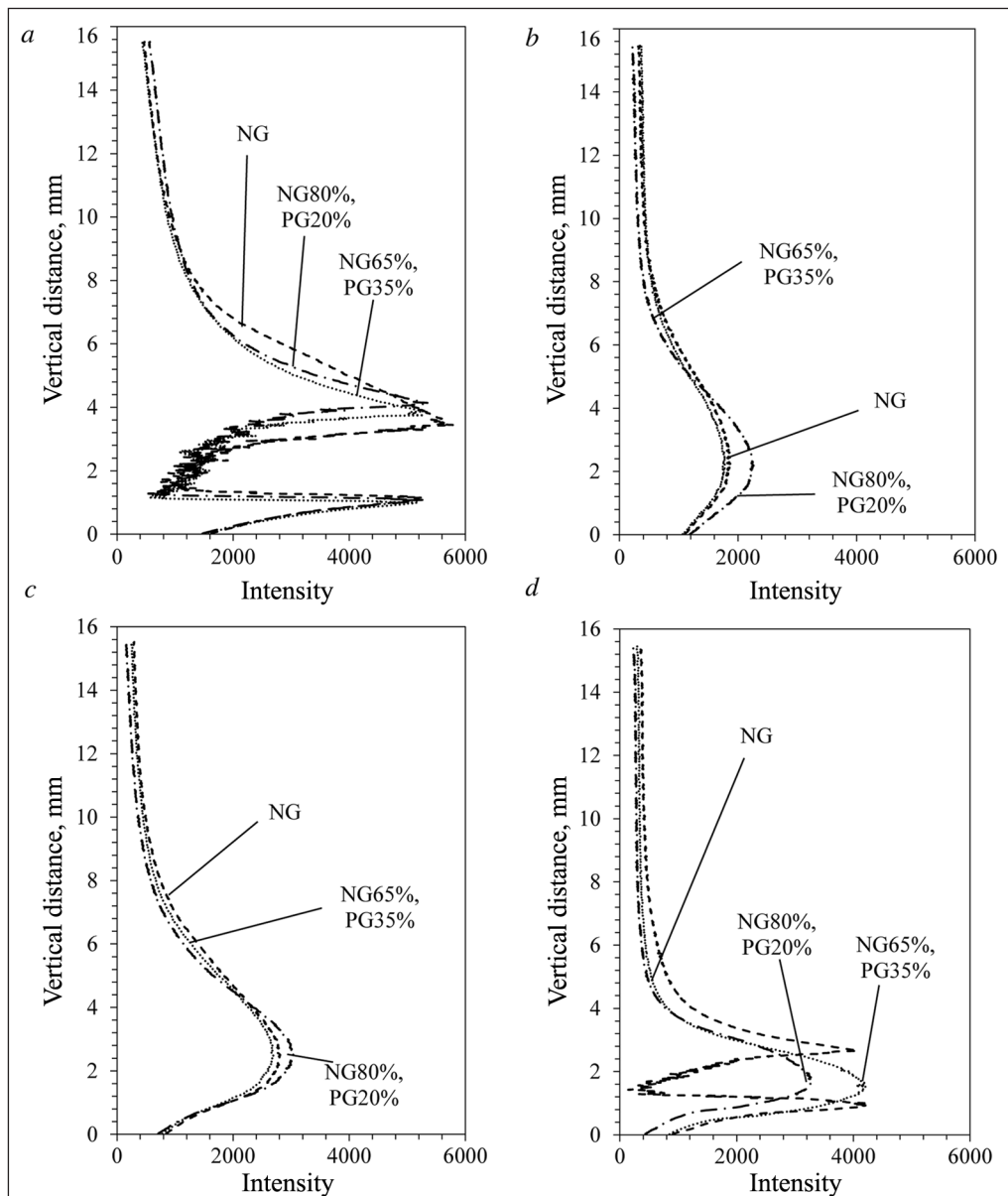


Fig. 4. The spectral profile along the flames as a function of distance above the burner and at  $\text{ER} = 1$  with different gas mixtures – natural gas (NG); 65% natural gas and 35% producer gas mixture (NG65%, PG35%); and 80% natural gas and 20% producer gas mixture (NG80%, PG20%): a –  $\text{CH}^*$  filter, at 431.4 nm;  $\text{ER} = 1.0$ ; b –  $\text{OH}^*$  filter, at 308.9 nm; c –  $\text{CH}^*$  filter, at 387.1 nm; d –  $\text{C}_2^*$  filter, at 514 nm

It was assumed that this effect was due to quenching in the zone between 1 and 3 cm from the burner nozzle. This assumption is based on observation of 514 nm wavelength peaks. When burning natural gas at ER = 1, two peaks at 1 cm and 3–5 cm distance from the burner nozzle disappear and only one extended peak can be observed. It is related to high  $C_2^*$  concentration. In that case, the flue gas analyser also shows high CO concentration (Table 5) that is related to  $C_2^*$  existence in the combustion zone [12]. That means that quenching disappears at observed conditions, but reappears when ER or fuel mixture composition is changed. Nabhani et al. [13]

mention that hydrogen addition to fuel mixture extends flame stability at very low and very high flow conditions. This can be a reason why quenching effect disappears at ER = 1.3 when using natural and producer gas mixture, but it does not happen when using only natural gas (Fig. 4d).

$NO_x$  reduction was observed when using gas mixture instead of pure natural gas at mixture proportions of 80% natural gas and 20% producer gas (Fig. 5). The reason of this effect also relates to the presence of hydrogen in the mixture. According to Andersson et al. [14], there are more than few researches stating that hydrogen addition to lean natural gas mixture lowers  $NO_x$  emissions [15].

Table 5. Results of flue gas analysis with a flue gas analyser TESTO 350 XL for all gas mixtures used in the experiments

Mixture	ER	CO, mg/m <sup>3</sup>	CO <sub>2</sub> , %	NO <sub>x</sub> , mg/m <sup>3</sup>
Natural gas	1	16 900	11	125
	1.1	150	11	150
	1.2	6	10	173
	1.3	4	10	198
Natural gas 80% + Producer gas 20%	1	920	12	155
	1.1	120	11	160
	1.2	54	10	173
Natural gas 65% + Producer gas 35%	1	2 600	11	118
	1.1	40	11	141
	1.2	5	11	149
	1.3	9	8	146

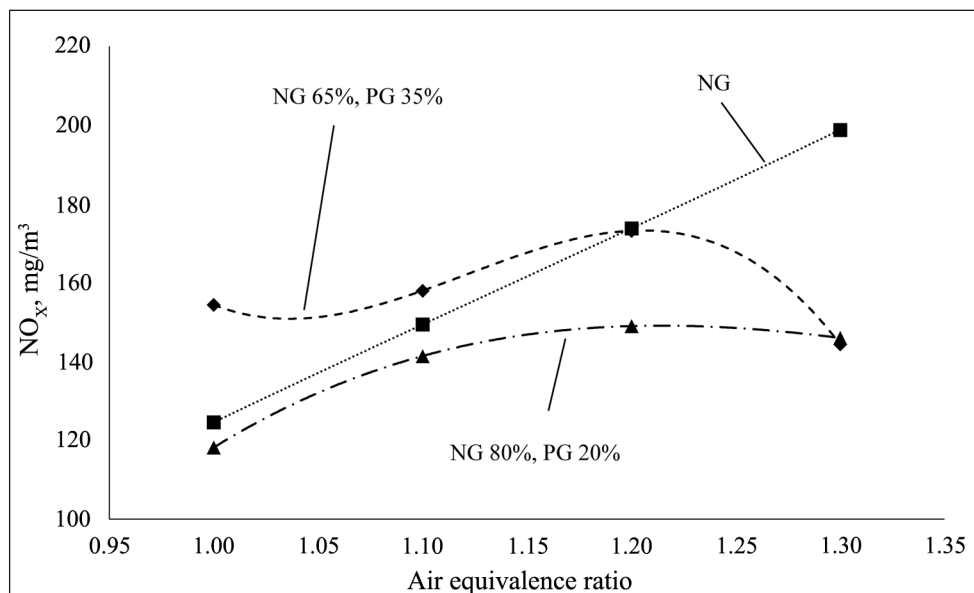


Fig. 5.  $NO_x$  emissions in flue gas during the experiment. NG – natural gas, PG – producer gas

Hydrogen presence in the mixture also explains the reason why in most of the plots of the current work a chemiluminescence intensity peak reaches the maximum closer to the burner. It means that the reactions related to the chemiluminescent intensity peak at a specific wavelength (see Table 1) start faster when using mixtures. According to Slim et al. [16], hydrogen reacts faster with oxidant than methane and increases temperature in the reaction zone, so the combustion reactions end faster and closer to the burner's nozzle. The chemiluminescence intensity shift toward the burner's nozzle can be seen in the results. The hydrogen presence in the mixture for combustion was confirmed with the VISIT analyzer data of producer gas composition (Table 6).

The relation between ER and the chemiluminescence intensity is reported in multiple articles [1, 2, 17]. This relation can also be seen in the present analysis. This linear dependency remains not only for pure natural gas but for the mixtures with producer gas as well (Fig. 6).

## CONCLUSIONS

Due to quenching in the zone between 1 and 3 cm from the burner nozzle, a single peak of the chemiluminescent species intensity in the flame was observed only at 308.9 and 387.1 nm wavelengths.

The examination of producer gas showed that it contains hydrogen. Presence of hydrogen in the gas mixture resulted in decreased  $\text{NO}_x$  emissions when burning natural gas with producer gas addition.

According to the reviewed literature and our research results, it can be stated that the shift of the chemiluminescence maximum intensity peak towards the burner nozzle was due to the presence of hydrogen in the producer gas. Hydrogen resulted in higher temperatures, and chemical reactions proceeded faster.

The excess ratio can be expressed as a function of  $\text{OH}^*/\text{CH}^*$  not only for natural gas but also for the mixture of natural gas and producer gas.

The relation determined from the flame image analysis can be conductive in developing a simple

Table 6. Average presence of hydrogen in the mixture for combustion, measured with a VISIT analyser. Content of producer gas in the gas mixture: 0%, 20%, 35%, respectively. NG – natural gas, PG – producer gas

ER	1	1.1	1.2	1.3
Mixture	Hydrogen, %			
NG	0	0	0	0
NG 80%, PG 20%	15.7	17.06	17.58	18.9
NG 65%, PG 35%	16.2	13.36	14.92	16.12

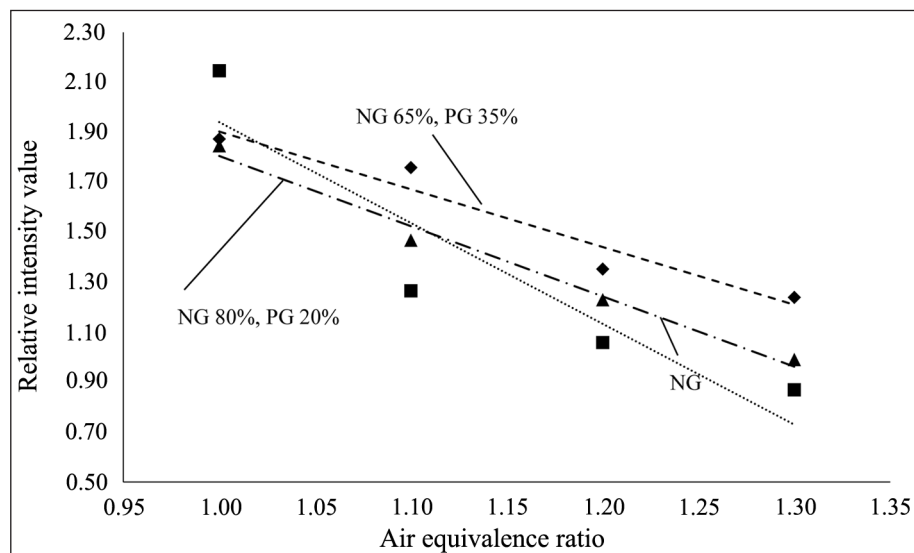


Fig. 6. Relation between the chemiluminescence intensity ratio of  $\text{OH}^*/\text{CH}^*$  and the air equivalence ratio; Content of producer gas in the gas mixture: 0%, 20%, 35%, respectively. NG – natural gas, PG – producer gas



nonintrusive monitoring and control system, based on optical flame imaging, implementing a burner that adapts automatically to varying composition of the gaseous fuel mixture and fuel and air flow rates, thereby ensuring the most favourable operating regime.

## ACKNOWLEDGEMENTS

This research is funded by the European Social Fund under the Project “Microsensors, Microactuators and Controllers for Mechatronic Systems (Go-Smart)” (Agreement No. VP1-3.1-ŠMM-08-K-01-015).

Received 17 July 2014

Accepted 4 December 2014

## References

1. Docquier N., Candel S. Combustion control and sensors: a review. *Progress in Energy and Combustion Science*. 2002. Vol. 28. No. 2. P. 107–150.
2. Hardalupas Y., Orain M., Panoutsos C. S., Taylor M. K., Olofsson J., Seyfried H., Richter M., Hult J., Aldén M., Hermann F., Klingmann J. Chemiluminescence sensor for local equivalence ratio of reacting mixtures of fuel and air (FLAMESEEK). *Applied Thermal Engineering*. 2004. Vol. 24. No. 11–12. P. 1619–1632.
3. Dribinsk V., Ossadtchi A., Mandelshtam V. A., Reisler H. Reconstruction of Abel-transformable images: The Gaussian basis-set expansion Abel transform method. *Review of Scientific Instruments*. 2002. Vol. 73. No. 7. P. 2634–2642.
4. Hardalupas Y., Orain M. Local measurements of the time-dependent heat release rate and equivalence ratio using chemiluminescent emission from a flame. *Combustion and Flame*. 2004. Vol. 139. P. 188–207.
5. Veríssimo A. S., Rocha A. M. A., Costa M. Operational, combustion, and emission characteristics of a small-scale combustor. *Energy & Fuels*. 2011. Vol. 25. No. 6. P. 2469–2480.
6. Bouvet N., Chauveau C, Go I., Lee S. Y., Santoro R. J. Characterization of producer gas laminar flames using the premixed gas burner configuration. *International Journal of Hydrogen Energy*. 2011. Vol. 36. P. 992–1005.
7. Higgins B., McQuay M. Q., Lacas F., Rolon J. C., Darabiha N., Candel S. Systematic measurements of OH chemiluminescence for fuel-lean, high-pressure, premixed, laminar flames. *Fuel*. 2001. No. 80. P. 67–74.
8. Ballester J., Garci'a-Armingol T. Diagnostic techniques for the monitoring and control of practical flames. *Progress in Energy and Combustion Science*. 2010. Vol. 36. P. 375–411.
9. Higgins B., McQuay M. Q. An experimental study on the effect of pressure and strain rate on CH chemiluminescence of premixed fuel-lean methane / air flames. *Fuel*. 2001. Vol. 80. P. 1583–1591.
10. Striūgas N., Zakarauskas K., Stravinskas G., Gri-gaitienė V. Comparison of steam reforming and partial oxidation of biomass pyrolysis tars over activated carbon derived from waste tire. *Catalysis Today*. 2012. Vol. 196. No. 1. P. 67–74.
11. Hernández J. J., Lapuerta M., Barba J. Flame stability and OH and CH radical emissions from mixtures of natural gas with biomass gasification gas. *Applied Thermal Engineering*. 2013. Vol. 55. No. 1. P. 133–139.
12. Kathrotia T. *Reaction Kinetics Modeling of OH\*, CH\*, and C<sub>2</sub>\* Chemiluminescence*. PhD Dissertation. Heidelberg: Ruprecht-Karls-Universität, 2011. P. 1–108.
13. Nabhani N., Sharifi V. Investigation on the combustion of hydrocarbon fuel enriched by hydrogen for a cleaner environment. *Proceedings of International Conference on Chemical, Environmental Science and Engineering (ICEEBS'2012), July 28–29, 2012, Pattaya, Thailand*. P. 35–39.
14. Andersson T. *Hydrogen Addition for Improved Lean Burn Capability on Natural Gas Engine*. Report SGC 134. 2002.
15. Tunestål P., Christensen M., Einewall P., Andersson T. *Hydrogen Addition for Improved Lean Burn Capability of Slow and Fast Burning Natural Gas Combustion Chambers*. SAE Technical Paper. 2002. P. 7–8.
16. Slim B. K., Darmeveil H., Van Dijk G. H. J., Last D., Pieters G. T., Rotink M. H., Overdiep J. J., Levinsky H. B. Should we add hydrogen to the natural gas grid to reduce CO<sub>2</sub> emissions? (Consequences for gas utilization equipment). *Proceedings of 23rd World Gas Conference, Amsterdam, 2006*. P. 1–15.

17. Hardalupas Y., Panoutsos C. S., Skevis G., Taylor A. M. K. P. Numerical evaluation of equivalence ratio measurement using OH\* and CH\* chemiluminescence in premixed iso-octane / air flames. *Proceedings of the European Combustion Meeting 2005*. P. 1–6.

**Andrius Saliamonas, Robertas Navakas,  
Nerijus Striūgas, Algis Džiugys,  
Kęstutis Zakarauskas**

### **GENERATORINIŲ DUJŲ PRIEMAIŠŲ ĮTAKA GAMTINIŲ DUJŲ LIEPSNOS SPEKTRINĖMS CHARAKTERISTIKOMS**

*Santrauka*

Straipsnyje pristatomi rezultatai, gauti analizuojant liepsną emisinės spektroskopijos būdu, registruojant chemiliuminescencinius radikalus OH\*, CH\* ir C<sub>2</sub>\*, kurie, kaip žinome, yra pagrindiniai angliavandenilių skilimo liepsnoje rodikliai. Tyrimo tikslas buvo ištirti, kokią įtaką generatorinių dujų priemaiša gamtinėse dujose turi liepsnos spektrinėms charakteristikoms

bangų ilgiuose, atitinkančiuose OH\*, CH\* ir C<sub>2</sub>\* radikalų susidarymo reakcijas, kai oro pertekliaus koeficientas kinta nuo 1,0 iki 1,3. Atlikti gamtinių dujų ir generatorinių dujų mišinių bandymai. Generatorinės dujos buvo pagamintos iš medienos granulijų laboratoriniame dujinimo reaktoriuje. Išanalizavus chemiliuminescencijos junginių intensyvumo pasiskirstymo išilgai degiklio vertikalios ašies profilius, nustatyta, kad esant tam tikroms sąlygoms degimo zonoje pasireiškia gesimas. Be to, esant generatorinių dujų priemaišoms, chemiliuminescencijos intensyvumas pasislenka link degiklio žiočių. Pastebėta tiek gamtinių dujų, tiek dujų mišinių tikėtina koncentracijų santykio OH\*/CH\* priklausomybė nuo oro pertekliaus koeficiento. Gauti rezultatai, naudojant įprastinę liepsnos emisinę spektroskopiją, gali būti pritaikomi degimo proceso optiniam stebėjimui ir valdymui.

**Raktažodžiai:** gamtinės dujos, degimas, chemiliuminescencija, atsinaujinantys energijos šaltiniai, spektroskopija